



Electron- and photon-induced plasmonic excitations in two-dimensional silver nanostructures

C. V. Hoang, M. Rana, and T. Nagao

Citation: [Applied Physics Letters](#) **104**, 251117 (2014); doi: 10.1063/1.4885387

View online: <http://dx.doi.org/10.1063/1.4885387>

View Table of Contents: <http://scitation.aip.org/content/aip/journal/apl/104/25?ver=pdfcov>

Published by the [AIP Publishing](#)

Articles you may be interested in

[Switchable plasmon-induced transparency in gold nanoarrays on vanadium dioxide film](#)

J. Vac. Sci. Technol. B **31**, 06FE01 (2013); 10.1116/1.4826561

[Self-aligned epitaxial metal-semiconductor hybrid nanostructures for plasmonics](#)

Appl. Phys. Lett. **98**, 243110 (2011); 10.1063/1.3596460

[Plasmonic effects and visible light diffraction in three-dimensional opal-metal photonic crystals](#)

Appl. Phys. Lett. **90**, 171108 (2007); 10.1063/1.2724894

[Metal-enhanced chemiluminescence: Radiating plasmons generated from chemically induced electronic excited states](#)

Appl. Phys. Lett. **88**, 173104 (2006); 10.1063/1.2195776

[Narrow plasmonic/photonic extinction and scattering line shapes for one and two dimensional silver nanoparticle arrays](#)

J. Chem. Phys. **121**, 12606 (2004); 10.1063/1.1826036

Agilent's Electronic Measurement Group is becoming **Keysight Technologies**.



Engineering Education & Research Resources DVD 2014

Agilent is the key to your test and measurement needs **Order yours**



The advertisement features a red header with the text 'Agilent's Electronic Measurement Group is becoming Keysight Technologies.' Below this is a row of ten colorful icons representing various engineering and research fields: a green Wi-Fi symbol, a blue checkmark, a blue graduation cap, a green book, a yellow sun, a green network diagram, a blue antenna, a purple microchip, a green wave, an orange vertical bar, and a red starburst. To the left of these icons is a circular image of the DVD cover, which is blue and white with the text 'Agilent Technologies Engineering Education & Research Resources DVD 2014'. Below the icons is the main title 'Engineering Education & Research Resources DVD 2014' in bold black text, followed by the slogan 'Agilent is the key to your test and measurement needs' and a red button with white text that says 'Order yours'. At the bottom is a blue banner with the Agilent Technologies logo and the company name.

Electron- and photon-induced plasmonic excitations in two-dimensional silver nanostructures

C. V. Hoang,^{1,a)} M. Rana,¹ and T. Nagao^{1,2,b)}

¹International Center for Materials Nanoarchitectonics (MANA), National Institute for Materials Science, 1-1 Namiki, Tsukuba 305-0044, Japan

²CREST, Japan Science and Technology Agency, 4-1-8 Honcho, Kawaguchi, Saitama 332-0012, Japan

(Received 16 March 2014; accepted 15 June 2014; published online 26 June 2014)

Plasmons are the quasi particles of collective oscillations of electrons and form the basis of plasmonics and optical metamaterials. We combined electron spectroscopy and optical spectroscopy techniques to study plasmons in atomically smooth Ag films and in epitaxial Ag nanodisks to map the momentum-energy dispersion curves of the two-dimensional (2D) sheet plasmon and the quasi-2D plasmons to clarify the essential differences between them. Our experimental results combined with the results of numerical electromagnetic simulations showed that the bulk-like nature of the silver plasmon starts in layers that are only two atoms thick. © 2014 AIP Publishing LLC.

[<http://dx.doi.org/10.1063/1.4885387>]

The energy-momentum dispersion of plasmons is one of the most important concepts in plasmonics, from which we can understand the origin of the spectral features and the frequency dependence of the interactions between the plasmonic nano-objects and light. This concept thus provides us with a profound understanding of the fundamental characteristics of plasmonic nanosystems, which can lead to the development of innovative nanophotonic devices.¹ In the dispersion curves of metal surface plasmons, the low momentum region in the near to mid-infrared (IR) region is conventionally accessed by optical means, such as the attenuated total reflection (ATR) technique, because the dispersion curve location is rather close to the light line. However, the higher energy-momentum region (above 0.01 \AA^{-1}) is only accessible by the use of the inelastic scattering of the charged particles, which has sufficient momentum in the \AA^{-1} region.²⁻⁴ It is therefore desirable to combine these two complimentary schemes to explore and increase our understanding of plasmonic materials. In particular, when the dispersion curve of a quasi-two-dimensional (2D) film deviates away from the light line in the higher wavenumber region, the “slow-light” nature of confined electromagnetic waves with propagation wavelengths in the angstrom region becomes increasingly prominent.^{2,3,6} In contrast, when the lateral dimension of a thin metal object becomes finite, a strong resonance would occur at a specific frequency so that the light can be absorbed and scattered strongly. This phenomenon is known as antenna resonance, and the surface charge density wave at this state will form standing waves, with a half-wavelength that roughly matches the size of the object.⁵⁻⁸ The “slow-light” standing waves supported by these low-dimensional nano-resonators often produce remarkable optical characteristics in the infrared region and are thus promising candidates for applications in infrared

telecommunications, bio-nanophotonics, waste heat management, and solar power generators.^{2,7,9}

This Letter is composed of two parts. In the first part, we report on the fabrication of flat 2D silver nanodisks supported by surfactant modified Si(111) substrates. The disks were prepared by physical deposition of silver on the substrates. Use of a two-step deposition process with different post-annealing temperatures enabled us to control the average size of the epitaxial Ag disks. The antenna-like optical resonance in the infrared region was varied systematically by changing the size and thickness of the disks, indicating the formation of the standing waves. In the second part of the Letter, these standing wave plasmons were used to construct the energy-momentum relation of the Ag plasmon and were compared with the propagating plasmons in Ag nanofilms, along with those in a monolayer silver film, which is known to be an ultimately thin pure 2D electron gas.¹² It is found that the nanometer-scale silver disks, which start from bilayer thicknesses,¹¹ already exhibit the properties of bulk-like plasmons (quasi-2D plasmons), which are described very well by the early theory of Ritchie when adopting bulk dielectric constants.^{13,14} However, the ultimately thin silver monolayer film exhibits the distinct features of a plasmon in a pure 2D quantum gas, as described by the theory of Stern.¹⁵

The experiments were performed under ultra-high vacuum (UHV) conditions, with a base pressure of 9×10^{-11} Torr. The chamber was equipped with a reflection high energy electron diffraction (RHEED) system to investigate the surface morphology of the nanostructure during growth. To measure the IR spectra, the chamber was coupled to a Fourier transform IR (FTIR) spectrometer (Nicolet-Japan NEXUS-670) with a mercury cadmium telluride detector via IR-transparent ZnSe windows. The spectrometer was thoroughly purged with nitrogen gas prior to the experiments. A lightly doped (resistivity of 0.5 \Omega-cm) Si(111) wafer was cleaned in an UHV with a standard procedure to obtain the Si(111)- 7×7 reconstruction.¹⁶ About 1/3 of a monolayer (ML) of In was then evaporated on the Si(111)- 7×7 room temperature (RT) substrate (hereafter referred to as Si- 7×7) and annealed at $500 \text{ }^\circ\text{C}$ for 30 s to form

^{a)}Present address: Institute of Materials Science, Vietnam Academy of Science and Technology, 18 Hoang Quoc Viet Street, Cau Giay District, Hanoi 10000, Vietnam.

^{b)}Author to whom correspondence should be addressed. Electronic mail: Nagao.Tadaaki@nims.go.jp

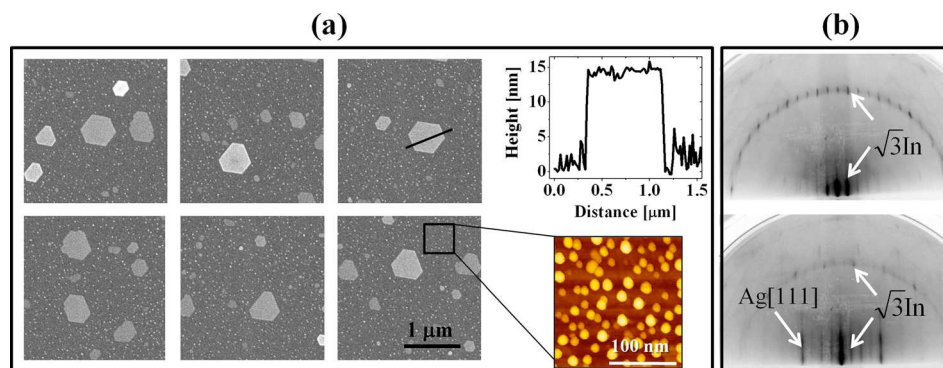


FIG. 1. (a) Scanning electron micrographs of typical silver nanodisks prepared on a reconstructed ($\sqrt{3}\text{In}$ phase) Si substrate; 3 ML of Ag were deposited on the substrate. The insets show the typical height profile taken from AFM (marked as the black line in the SEM image) and the residual small clusters scattered on the $\sqrt{3}\text{In}$ phase substrate. (b) The RHEED patterns of the bare $\sqrt{3}\text{In}$ before and after silver deposition (5 ML). Electron energy of 20 keV and a grazing angle of approximately 1° were used with respect to the Si substrate surface.

the $\text{Si}(111)\text{-}\sqrt{3} \times \sqrt{3}\text{-In}$ (referred to as $\sqrt{3}\text{In}$) reconstructed surface. Silver nanodisks were prepared by physical deposition of Ag on the $\sqrt{3}\text{In}$ substrate (which was maintained at RT during deposition), followed by annealing at approximately $70\text{--}80^\circ\text{C}$ for 3 min. The thickness of the In layer (and that of the Ag layer) was calibrated by monitoring the surface phase transition from the $\text{Si-}7 \times 7$ structure to the $\sqrt{3}\text{In}$ reconstruction (as observed by RHEED). One ML of In (and of Ag) corresponds to the $\text{Si}(111)$ substrate's topmost layer, with an atomic density of 7.84×10^{14} atoms/cm². The FTIR spectroscopic measurements were performed with 4 cm^{-1} resolution using the normal-incidence transmission geometry. Electromagnetic simulations based on the finite-difference time-domain (FDTD) method and rigorous coupled wave analysis (RCWA) were used to simulate the measured spectra. A broadband IR light source was used at normal incidence to illuminate the sample surface. The relative transmission spectrum was obtained by normalizing the spectra from the silver disks supported by the Si substrate with reference to spectra taken from bare Si samples.

Figure 1 shows the fabricated silver nanodisks after deposition and annealing of 3 ML of silver on the $\sqrt{3}\text{In}$ substrate, indicating that the majority of the nanodisks have hexagonal 2D shapes with epitaxial relationships with respect to the substrate. The typical disk has a diameter of about 500 nm and height of 15 nm, and smaller silver islands with diameters of less than 10 nm and heights of 4–6 nm are also observed (as shown by the zoomed-in picture from the atomic force microscope (AFM)). The disks are distributed uniformly over the entire $\sqrt{3}\text{In}$ surface. Figure 1(b) shows the electron diffraction patterns of the $\sqrt{3}\text{In}$ substrate before and after formation of the silver islands. The streaky and azimuthally anisotropic features in the diffraction pattern indicate the formation of single crystalline Ag(111) flat islands, as expected from the epitaxial islands shown in Fig. 1(a). Figure 2(a) shows the evolution of the measured transmission spectra of the disks (2 ML of silver were initially deposited) as a function of the annealing time at 70°C . The 100% line shows the initial transmittance of the $\sqrt{3}\text{In}$ substrate prior to silver deposition. The relative transmittance of the as-deposited silver film (with respect to that of the $\sqrt{3}\text{In}$ substrate) shows a significant reduction, but the prominent resonance in the mid-IR range is not found in this case (brown curve). This can be attributed to

the formation of Ag clusters (see the lower right section of Fig. 1(a)), which produces the broad Mie plasmon-like feature trailing from the visible to the near-infrared region. However, after the substrate was annealed at 70°C for 30 s, the sample gives a clear resonance at around 350 meV

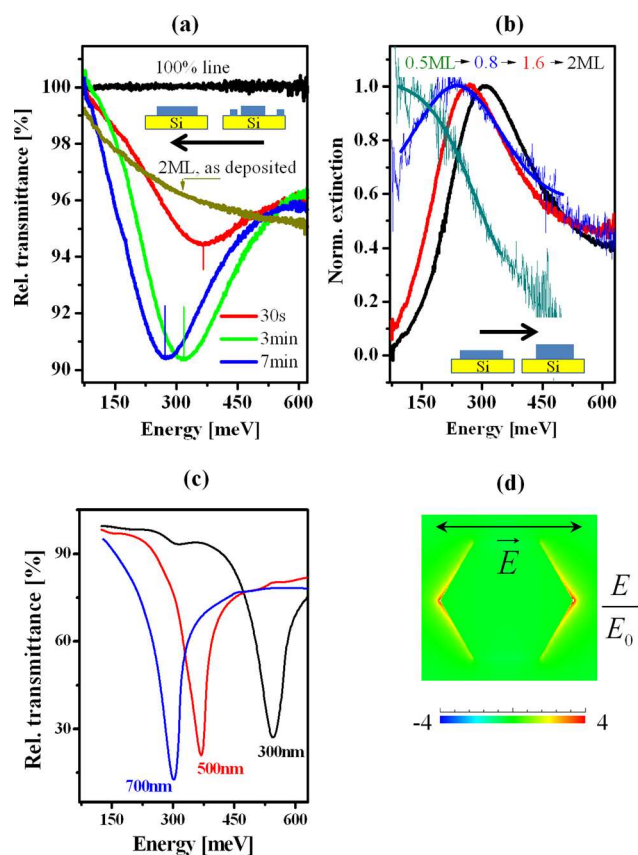


FIG. 2. Spectroscopic measurements (infrared spectroscopy) and numerical calculation results (RCWA, FDTD method) of the optical properties of the fabricated nanodisks. (a) The evolution of the antenna-like plasmonic resonance of the nanodisks. The brown curve shows the transmittance of the as-deposited silver film, while the remainder shows the systematic shift of the strong resonance feature versus the sample annealing time. (b) The blueshift of the resonance as a function of the silver thickness. (c) The RCWA calculation results for various disk dimensions, ranging from 300 nm to 700 nm. The disk thickness remains constant at 15 nm. (d) FDTD simulation results of the electric field distribution over a typical silver disk when excited at its resonance wavelength in the infrared region ($4\ \mu\text{m}$).

(plotted as a red curve). Upon further annealing at 70 °C for up to 7 min, a systematic redshift of the resonance is observed, from 350 meV to 270 meV. Because appropriate thermal treatment drives the diffusion of the small silver clusters and their absorption into the larger silver islands via Ostwald ripening, the observed spectral shift is assigned to the shift in the antenna-like resonance (dipolar resonance) of the silver islands. The thermally induced evolution of the surface morphology is also observed by scanning electron microscopy (SEM) and by RHEED; e.g., the diffraction of the Ag(111) islands becomes more dominant as the crystallinity and size of the islands increase. A similar spectral shift is also observed as a function of the silver thickness, as shown in Fig. 2(b). Here, we present the results in the form of a normalized extinction to emphasize the features stemming from the antenna-like resonances. In contrast to the effect of the increased annealing time, an increase in the silver coverage produces a blueshift. This is correlated to the increased thickness of the hexagonal disks, which leads to the increased plasmon resonance frequency, as expected from the theory of ultrathin-film plasmons.¹³ The systematic behavior observed above shows good agreement with the scenario of the antenna resonance, or the standing wave plasmon, for the ultrathin Ag disks.

To further understand these phenomena, electromagnetic simulations based on the RCWA and FDTD methods were performed, with results as shown in Figs. 2(c) and 2(d), respectively. In these simulations, the disk thickness remains constant at 15 nm, while the lateral dimensions of the disks (along the longer axis) are varied from 300 nm to 700 nm. Consistent behavior is found (although a slight deviation of ~40 meV exists between measurements) and gives clear confirmation of the antenna-like (standing-wave plasmon) origin of the strong resonance of the Ag nanodisks that we found in the experiments. Figure 2(d) clearly shows the dipolar resonance feature of the Ag disks (500 nm diameter and 15 nm thickness) excited at the resonance wavelength (4 μm) with a strong electric field enhancement at the disk perimeter.

Because the standing wave plasmon of a finitely sized closed structure assumes the features of dipolar resonance,^{6,10} it is expected that the resonance energy will mainly depend on the sizes of the objects and the dielectric screening effect of the surrounding medium.⁶ For a nano-scale object with a lateral dimension d , the plasmon wavevector is written as $q = \pi/d$ for the case of fundamental resonance.^{16,17} Because the disk dimensions have been measured by SEM and the plasmon energy has been measured by IR spectroscopy (IRS), the energy-momentum relationship can be constructed experimentally. We can estimate the dispersion curve of the propagating plasmons in quasi-2D ultrathin Ag films using Ritchie's theory.^{12,13} Dispersion of this infinitely extended quasi-2D film can be calculated using the equation shown below for the three-slab Si/Ag/vacuum model

$$e^{2qh} = \frac{[\epsilon_{\text{Si}}(\omega) - \epsilon_{\text{Ag}}] \cdot [\epsilon_{\text{Si}}(\omega) - \epsilon_{\text{Vac}}]}{[\epsilon_{\text{Si}}(\omega) + \epsilon_{\text{Ag}}] \cdot [\epsilon_{\text{Si}}(\omega) + \epsilon_{\text{Vac}}]}, \quad (1)$$

where h is the thickness of the silver layer; ϵ_{Si} , ϵ_{Ag} , and ϵ_{Vac} are the dispersive bulk three-dimensional (3D) dielectric

functions of the three elements of the structure, i.e., silicon, silver, and the vacuum (where $\epsilon_{\text{Vac}} = 1$), respectively.¹⁸

In contrast, for a pure 2D film composed of a metal monolayer with single-atom-thickness, a qualitatively different plasmon dispersion is expected where the hydro-dynamic continuum model using bulk dielectric functions is no longer valid.^{15,19} It was proven previously that the dispersion in such a system is precisely described by Stern's non-analytical formula, which can be approximated as follows within a small q limit:^{12,15,20}

$$\omega_{2D}(q) = \left[\frac{4\pi N_{2D} \cdot e^2}{m^*} \cdot \frac{|q|}{1 + \epsilon_{\text{Si}}} + \frac{6 N_{2D} \cdot \hbar^2 \cdot \pi}{(2m^*)^2} \cdot |q|^2 \right]^{1/2}, \quad (2)$$

where N_{2D} is the electron density of the film, and m^* is the effective mass of the 2D electron gas. In particular, the monolayer silver film supported by the Si surface has a Fermi wavelength of electrons of the order of $\lambda_F \sim 5$ nm, which is one order of magnitude higher than that of the bulk 3D Ag, which means that thickness of the confining medium (one atom thick in this case) is far smaller than the wavelengths of the conduction electrons of this system.^{12,19,20} This situation produces the ideal 2D behavior of the plasma oscillation of the electrons because of the extremely strong 2D confinement when compared with that of the multilayer quasi-2D Ag films.^{12,20} The best quantitative fit for the propagating plasmon in the Ag monolayer ($\sqrt{3} \times \sqrt{3}$ -Ag phase) on Si was achieved with the following fitting parameters:¹² $N_{2D} = 1.9 \times 10^{13} \text{ cm}^{-2}$ and $m^* = 0.3 \times m^*$ (where m^* is the free-electron mass). The fitting results reflect the intrinsic 2D electronic nature of the Ag monolayer that originates from the intermixed Ag-Si 2D atomic arrangement and that yields a free-electron-like 2D metallic band near the Fermi level.

In Fig. 3, we show the energy-momentum dispersions of the Ag ultrathin films/disks that were grown on the silicon substrates: a single ML Ag film (solid red circles),¹² previously reported bi-layer Ag disks (solid black circles),¹¹ 15 nm

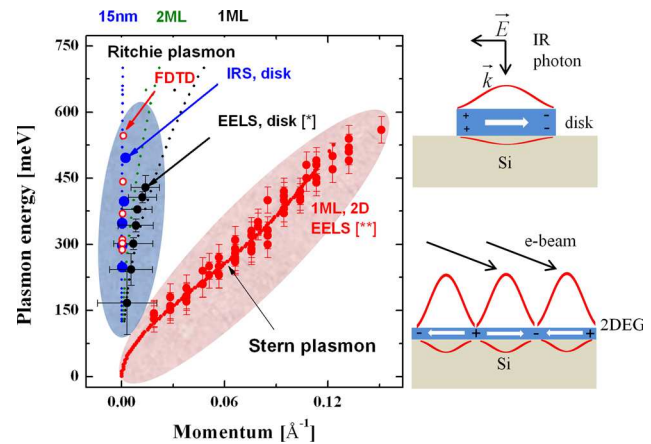


FIG. 3. A comprehensive plot of the dispersion curves obtained from the different excitation regimes on the silver nanodisks and 2D films. The right insets show schematic illustrations of the excitation mechanisms using photons (upper) and electrons (lower). The photon-based excitation is performed for finite-sized Ag disks, which exhibit antenna resonance. EELS data, which were reported in the literature, are plotted for the flat ultrathin bi-layer silver disk¹¹ and monolayer Ag film¹² (noted as [*] and [**], respectively).

thick Ag disks (IRS measurement data, red open circles), and the results of the corresponding FDTD simulations (solid blue circles). The theoretical calculations from the Ritchie and Stern models are also plotted in the same figure, as indicated by the small dots and the bold red curve, respectively. It is shown that the dispersion curve that was constructed from the standing wave plasmons measured from the 15 nm thick nanodisks is very steep and follows the three-slab model of the Ritchie plasmon reasonably well. The dispersion measured reported previously by electron energy loss spectroscopy (EELS) for the bi-layer Ag disks also follows Ritchie's dispersion and is located only slightly below the calculated dispersion for the 2 ML film, which may indicate that these Ag disks possessed bulk-like atomic structures with slight electron charge transfers to the substrate.¹¹ In contrast, for the case of a 1 ML thick film (fabricated by the direct deposition of Ag onto the annealed Si(111) surface) where strong confinement of the electrons in the 2D space is expected, a significant difference is found between the Ritchie plasmon (denoted by the black dotted curve) and the experimental results reported from EELS (bold red curve), such as a dramatically reduced phase velocity and a characteristic frequency upshift at high wavenumbers.^{12,19} This monolayer plasmon fits Stern's non-analytical dispersion curve precisely and thus is unambiguously assigned to the pure 2D mode or "sheet plasmon" of an electron gas that is confined in a sufficiently thin system compared to its own Fermi wavelength, while exhibiting qualitative differences from the "quasi-2D" Ritchie plasmons.^{11,13,21} This difference originates from the differences in the nominal sheet electron density and those in the three-dimensional coulombic interaction that was induced by the charge density oscillation, where, in the former case, the polarization in the vertical direction is absent.

In conclusion, we have performed a comprehensive study of plasmons confined in ultrathin films and disks using combined electron spectroscopic and optical spectroscopic measurements in the mid-infrared region. We found that the behavior of the standing wave plasmons of the ultrathin Ag nanodisks with thicknesses of more than two atomic layers follows the hydro-dynamic Ritchie theory when adopting bulk three-dimensional dielectric functions with specific thicknesses. In contrast, the plasmon in the ultimately thin (one-atom-thick) Ag film does not follow the formula of the Ritchie plasmon and can only be described using Stern's non-analytical dispersion curve for the pure 2D electron system.

The proposed methodology presented here will provide profound insights into the behavior of plasmons that are confined in ultimately thin systems and will also provide useful information for the application of these plasmons to infrared nanophotonics.

This work was supported by a Grant-in-Aid for Scientific Research (KAKENHI) from the Japan Society for Promotion of Science (JSPS) and by the World Premier International Research Center Initiative on "Materials NanoArchitectonics" from the Ministry of Education, Culture, Sports, Science and Technology (MEXT, Japan). C.V.H. was supported from the Fellowship Program of JSPS.

- ¹W. L. Barnes, A. Dereux, and T. W. Ebbesen, *Nature* **424**, 824 (2003).
- ²T. Nagao, G. Han, C. V. Hoang, J.-S. Wi, A. Pucci, D. Weber, F. Neubrech, V. M. Silkin, D. Enders, O. Saito, and M. Rana, *Sci. Technol. Adv. Mater.* **11**, 054506 (2010).
- ³T. Nagao, S. Yaginuma, T. Inaoka, and T. Sakurai, *Phys. Rev. Lett.* **97**, 116802 (2006).
- ⁴H. Ibach, *Surf. Sci.* **66**, 56 (1977).
- ⁵H. Okamoto and K. Imura, *Prog. Surf. Sci.* **84**, 199 (2009).
- ⁶L. Novotny, *Phys. Rev. Lett.* **98**, 266802 (2007).
- ⁷S. Kawata, *Jpn. J. Appl. Phys., Part 1* **52**, 010001 (2013).
- ⁸C. Wu, A. B. Khanikaev, R. Adato, N. Arju, A. A. Yanik, H. Altug, and G. Shvets, *Nature Mater.* **11**, 69 (2012).
- ⁹C. V. Hoang, M. Oyama, O. Saito, M. Aono, and T. Nagao, *Sci. Rep.* **3**, 1175 (2013).
- ¹⁰L. Ju, B. Geng, J. Horng, C. Girit, M. Martin, Z. Hao, H. A. Bechtel, X. Liang, A. Zettl, Y. Ron Shen, and F. Wang, *Nat. Nanotechnol.* **6**, 630 (2011).
- ¹¹H. Qin, Y. Gao, J. Teng, H. Xu, K.-H. Wu, and S. Gao, *Nano Lett.* **10**, 2961 (2010).
- ¹²T. Nagao, T. Hildebrandt, M. Henzler, and S. Hasegawa, *Phys. Rev. Lett.* **86**, 5747 (2001).
- ¹³R. Ritchie, *Surf. Sci.* **34**, 1 (1973).
- ¹⁴*Electron Energy Loss Spectroscopy and Surface Vibrations*, edited by H. Ibach and D. L. Mills (Academic, San Francisco, 1982).
- ¹⁵F. Stern, *Phys. Rev. Lett.* **18**, 546 (1967).
- ¹⁶H. V. Chung, C. J. Kubber, G. Han, S. Rigamonti, D. Sanchez-Portal, D. Enders, A. Pucci, and T. Nagao, *Appl. Phys. Lett.* **96**, 243101 (2010).
- ¹⁷F. Neubrech, T. Kolb, R. Lovrincic, G. Fahsold, A. Pucci, J. Aizpurua, T. W. Cornelius, M. E. Toimil-Molares, R. Neumann, and S. Karim, *Appl. Phys. Lett.* **89**, 253104 (2006).
- ¹⁸E. D. Palik, *Handbook of Optical Constants in Solids* (Academic Press, 1997).
- ¹⁹T. Nagao, *Oyo Buturi* **73**(10), 1312 (2004), available at <https://www.jsap.or.jp/ap/2004/10/ob731312-e.xml>.
- ²⁰T. Nagao, in *Dynamics at Solid State Surfaces and Interfaces Part II*, edited by U. Bovensiepen, H. Petek, and M. Wolf (Wiley-VCH Verlag GmbH, Berlin, 2010), pp. 189–211.
- ²¹F. Moresco, M. Rocca, T. Hildebrandt, and M. Henzler, *Phys. Rev. Lett.* **83**, 2238 (1999).